Enhancing Brain-Tumor Imaging Using a Robust Deep-Learning Approach for Noise Removal and Image Clarity

V. H. Shruti
Department of Electronics and Communication Engineering, Sharnbasva University, Kalaburagi, India
vhshruthiresearch@gmail.com (corresponding author)

Lakshmi Patil
Department of Electronics and Communication Engineering, Sharnbasva University, Kalaburagi, India
patillakshmi192@gmail.com

Received: 3 October 2025 | Revised: 26 December 2025 | Accepted: 6 January 2026

 DOI: https://doi.org/10.48084/etasr.15294

ABSTRACT

Medical imaging plays a crucial role in the diagnosis of brain tumors. However, the presence of noise, such as Gaussian and Rician noise, degrades image quality, affecting diagnostic accuracy. Existing denoising methods struggle to effectively remove noise without sacrificing critical image details, limiting their usefulness in clinical applications. Hence, this study develops a robust denoising model that preserves essential anatomical structures while efficiently removing noise from brain-tumor images. The study proposes a Three-Layer Convolutional Neural Network (TL-CNN) model to denoise brain-tumor images. The proposed TL-CNN model was trained and tested on the Brain Tumor Segmentation (BraTS) 2021 medical imaging dataset, and evaluated using the Peak Signal-to-Noise Ratio (PSNR). The TL-CNN outperformed existing approaches, achieving a PSNR of 39.84 dB, which demonstrates its superior ability to suppress noise while preserving critical anatomical details. Compared with Zero Contrast-Enhanced Magnetic Resonance Imaging (ZeroCEMR) approach variants, including U-Net Reconstruction Encoder (UNetRe), Cross-Modal U-Net Reconstruction Encoder (CUNetRe), and YOLO-based Reconstruction Encoder (YOLORe), the TL-CNN achieved improvements of 20.34%, 13.15%, and 5.07% in PSNR, respectively. Furthermore, in comparison with the Permutate U-Net combined with Principal Component Analysis (PCA), TL-CNN demonstrated an 11.3% improvement in PSNR. Additional evaluations across different noise types and varying noise levels confirmed the robustness of TL-CNN, which consistently delivered superior denoising performance and maintained high structural fidelity under diverse imaging conditions.

Keywords-brain tumor; image denoising; CNN; medical imaging; noise reduction; PSNR

I. INTRODUCTION

Brain tumors are among the most critical neurological disorders, arising from abnormal cell growth within the brain and leading to severe cognitive, functional, and life-threatening complications. These tumors may originate within the brain itself (primary tumors) or spread from other organs (secondary or metastatic tumors) [1]. Depending on their location and severity, brain tumors can impair motor control, memory, speech, and personality, and in extreme cases may result in mortality. Early and accurate diagnosis is therefore essential for effective treatment planning and improved patient survival. Medical imaging modalities, such as Magnetic Resonance Imaging (MRI) and Computed Tomography (CT), play a significant role in identifying tumor presence, size, and progression. However, image quality is often degraded by noise, motion artifacts, and acquisition limitations, which complicate tumor detection, segmentation, and classification tasks. Noise contamination may obscure lesion boundaries, mislead clinical interpretation, and negatively impact automated analysis systems, leading to inaccurate diagnosis or delayed treatment [2]. To overcome these challenges, Artificial Intelligence (AI), particularly Machine Learning (ML) and Deep Learning (DL), has emerged as a powerful solution in medical image analysis. DL-based methods can automatically learn complex hierarchical features, enable accurate tumor detection, segmentation, and classification, reducing dependency on manual interpretation [3-12]. DL models frequently outperform traditional image processing techniques in both accuracy and computational efficiency, making them highly suitable for clinical applications.

DL-based solutions for brain tumor analysis have been explored. In [1], a comprehensive review of 142 MRI-based studies published between 2020 and 2023 was conducted, with 20 of them selected for detailed evaluation. The study highlighted the effectiveness of Convolutional Neural Networks (CNNs) and related architectures in automatically extracting discriminative features from MRI data, achieving high accuracy in tumor classification. However, there were challenges related to noise robustness and generalization across datasets. In [3], an automated biopsy planning framework was proposed using MRI and Magnetic Resonance Angiography (MRA) data. The method proposed in [4] employed cortical surface extraction, tumor localization, vascular segmentation, and trajectory planning, evaluated on the ITKTubeTK dataset. While this approach improved reproducibility and reduced manual intervention, its reliance on high-quality input images limited its robustness under noisy conditions. Further efforts focused on enhancing image quality before segmentation. In [5], a hybrid approach using Wavelet Packet Transform (WPT) and Linear Minimum Mean Square Error (LMMSE) filtering was proposed to suppress noise, followed by Fast C-Means clustering for segmentation. Evaluated on the BraTS 2021 dataset, the method achieved strong performance in terms of PSNR, Structural Similarity Index Measure (SSIM), and Dice Similarity Coefficient (DSC). Despite its effectiveness, the approach relied heavily on handcrafted preprocessing techniques, which may not generalize well across diverse imaging conditions. Similarly, in [6], CNN, EfficientNet, and Swin Transformer models were employed for multi-class brain tumor classification using MRI data. EfficientNet achieved the highest accuracy of 98.72%, demonstrating the potential of modern architectures. However, these models are sensitive to noise and often depend on extensive preprocessing pipelines.

Dataset evolution has also played a crucial role in advancing brain tumor analysis. Authors in [8] reviewed the evolution of the BraTS datasets from 2012 to 2024, highlighting improvements in annotation quality, data diversity, and clinical relevance. While these datasets significantly enhanced segmentation performance, challenges related to noise robustness and domain variability persist. Similarly, advancements in medical image super-resolution were reviewed in [9], where Generative Adversarial Networks (GANs), CNNs, Transformers, and diffusion models were explored to improve diagnostic image quality. Although these methods enhanced visual clarity, limitations related to evaluation consistency, robustness, and real-world deployment were identified. Efforts have also focused on reducing reliance on contrast agents. In [10], the ZeroCEMR approach was introduced to synthesize contrast-enhanced MRI images without Gadolinium-Based Contrast Agents (GBCAs). Using multi-modal inputs and attention mechanisms, the model achieved high PSNR values up to 37.82. However, such approaches remain computationally complex and sensitive to noise in input modalities. Similarly, in [11], the CARE-MRI model employed a Dual Channel-Hint Residual Network to enhance MRI denoising, achieving high PSNR and SSIM values. Despite its strong performance, the approach requires carefully tuned architectures and may struggle with generalization across diverse datasets. In [12], MRI Positron Emission Tomography (PET) fusion using PCA and a Permutate U-Net achieved improved segmentation accuracy on BraTS datasets, yet the effectiveness of segmentation remained dependent on the quality of fused images and preprocessing accuracy.

Research on brain-tumor imaging can be broadly categorized based on the underlying techniques. CNN-based methods [1, 3, 6] have demonstrated strong performance in tumor detection, segmentation, and classification by automatically extracting hierarchical features from MRI data. However, these models often struggle with noise robustness and require extensive preprocessing. GAN-based and super-resolution approaches [9] enhance image quality and clarity, improving visualization of fine tumor details. Nevertheless, they tend to be computationally intensive and sensitive to training instability. Hybrid optimization and filtering methods [5, 12], such as WPT with LMMSE or PCA-fused U-Nets, integrate signal processing with DL to suppress noise, yet they rely heavily on handcrafted feature extraction and may not generalize well across datasets. Finally, contrast-agent reduction approaches [10, 11] focus on synthesizing contrast-enhanced images without GBCAs, improving patient safety, but these methods are sensitive to input noise and require complex architectures. Collectively, while these studies have advanced brain-tumor imaging, they reveal persistent limitations in noise suppression, structural fidelity, and cross-dataset generalization, motivating the development of a robust, end-to-end denoising approach like the proposed TL-CNN. The latter is specifically designed for noise removal in brain tumor imaging. It focuses on enhancing MRI and CT images by effectively suppressing noise while preserving critical structural and textural details. Unlike conventional methods, the proposed approach integrates noise reduction directly into the learning framework, improving downstream tumor segmentation and classification performance. The contributions of TL-CNN are:

- The development of a TL-CNN architecture designed for robust noise removal in brain tumor images.
- Introduction of a novel feature extraction strategy that enhances structural clarity while minimizing information loss.
- A comprehensive comparative evaluation against state-of-the-art denoising techniques, demonstrating superior performance.

By addressing noise-related limitations in existing approaches, the proposed TL-CNN provides a more reliable and efficient foundation for accurate brain tumor analysis and clinical decision-making.

II. METHODOLOGY

This study presents a TL-CNN approach to improve brain-tumor images. The structured organization ensures clarity and facilitates a comprehensive understanding of the proposed methodology. Figure 1 illustrates the TL-CNN architecture designed for denoising brain-tumor images.

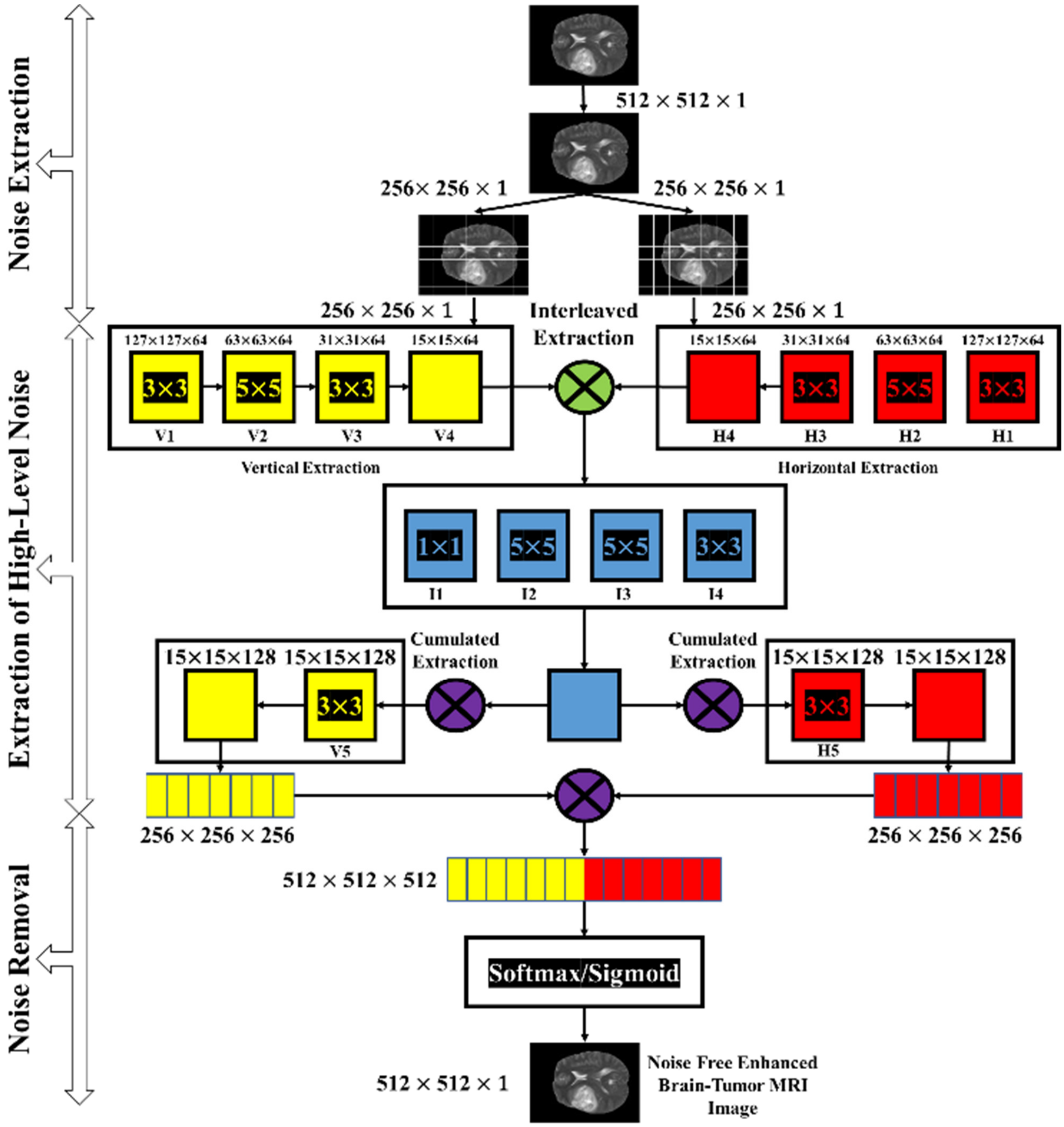

Fig. 1. Proposed TL-CNN architecture.

A. Architecture and Preprocessing

To remove noise and enhance brain-tumor images, first, the latter were standardized (pre-processing process). For preparing brain-tumor images in a standard format, the images were initially resized into 512×512 pixels. When an image is resized, its dimensions are changed (either scaled up or down). If the resized image is placed back onto the original image, there might be areas of the original image that are not covered by the resized image. These uncovered areas are called non-overlapping regions. Hence, to retain the complete brain-tumor image, a non-overlapping region was set as 8×8, i.e., 64 pixels.

In the first step of TL-CNN, noisy brain-tumor images serve as the input, with the network designed to handle various noise conditions. TL-CNN has three extraction processes: vertical extraction, horizontal extraction, and interleaved extraction. In horizontal extraction, the CNN processes the brain-tumor image pixels row by row, which is crucial for identifying noise patterns that might propagate horizontally across the image. This helps the network learn to recognize features such as edges or boundaries that might be distorted by noise along horizontal axes. The vertical extraction works similarly but scans the pixels column by column. This is particularly useful for capturing noise patterns or features that extend vertically in the brain-tumor images. By analyzing vertical noise variations, the network becomes more adept at recognizing and suppressing noise that might obscure key vertical structures in the brain-tumor images. In both horizontal and vertical extraction, convolutional layer filters were applied, i.e., 3×3, 5×5, which captured low-level features like edges and detected noise patterns in brain-tumor images.

This work utilized a space-filling curved approach for the extraction of the relationship between horizontal-extraction and vertical-extraction processes by including an interleaved extraction process in CNN [13]. The space-filling curved approach is employed to preserve spatial continuity and spatial dependency among neighboring pixels by mapping multidimensional image data into a one-dimensional traversal while maintaining locality. This enables more effective correlation between horizontal and vertical feature representations, thereby improving noise characterization and feature extraction in TL-CNN. The interleaved extraction alternates between pixels in a pattern that combines both horizontal and vertical directions.

This approach enables the network to capture diagonal or more complex noise patterns that may not be easily detected by purely horizontal or vertical extraction. The interleaved sequence allows for a more holistic view of the noise, ensuring that no part of the image remains unprocessed due to directional bias. Also, it consists of multiple convolutions with filters 1×1, 3×3, 5×5, each layer learning higher-level features and abstract patterns. Finally, the cumulated extraction aggregates information from all previous sequences, ensuring that the CNN has an understanding of the noise in the image. By accumulating pixel-wise data from horizontal, vertical, and interleaved extraction, the network creates a more robust and generalized noise-removal capability.

The cumulated extraction aids in the final refinement of the denoised brain-tumor images, enhancing the clarity of brain tumor regions and preserving essential details that might have been affected by noise. Moreover, the flattened output from the last cumulated extraction is passed through fully connected layers, where extracted features are combined, finalizing the denoising process. The softmax layer assists in classifying the image by determining the likelihood of a clean versus a noisy image. The final output is a denoised version of the brain-tumor images, making the tumor regions more distinguishable for diagnostic or segmentation tasks. Together, these pixel-wise extraction allows the TL-CNN architecture to capture noise in multiple dimensions and orientations, ensuring a more thorough denoising process. This combination of extraction significantly improves the network's ability to remove noise, resulting in higher-quality brain-tumor image outputs and better detection of brain tumor regions.

B. Noise Feature Extraction

The sample-feature extraction is challenging because it relies on data contained inside a specific brain-tumor image. However, by utilizing redundant-feature characteristics and sample-feature extraction across spatial regions, several existing approaches demonstrated that feature-extraction does not depend on brain-tumor images. Hence, for extracting noise from brain-tumor images, an interpolation approach was deployed. The latter considered a single pixel and its adjacent pixels and calculated the variance between them, taking into account an image-size of 256×256.

Moreover, the initial sample-features were extracted using minimum training-overhead considering a two-filtering extraction process, i.e., horizontal extraction 3×1 and vertical extraction 1×3, which were employed in the CNN kernel. After applying the filtering extraction process, the brain-tumor image was convoluted using a padding and a stride of 1, utilizing the extraction filters. Finally, the variance among nearby pixels in both filtering extraction processes, i.e., horizontal-extraction and vertical-extraction were utilized for building a residual map having a size of 256×256×1. For better training of the TL-CNN approach, this work has added Rician, Gaussian, and Salt and Pepper noise, similar to [5], during this process.

C. Extraction of High-Level Noise

For extracting high-level noise, the extracted noise from the previous stage was considered as input. Traditional noise detection models perform poorly because they consider extracting features and establish relationship pixel-wise in just a single direction or by considering both directions, which fails to extract important noise characteristics. Hence, this work considers sample-feature extraction in both horizontal and vertical structures, where weights are extracted from both structures. Both the horizontal-extraction and vertical-extraction structures had four-layers of convolution, i.e., convolution, batch-normalization, activation, and pooling layer. After extraction from both structures, the extracted features are merged and passed on to interleaved-extraction, which helps to collect the final sample-features that contain noise characteristics, and aid in removing noise and reconstructing brain-tumor images.

The interleaved-extraction approach also has four layers of convolution, namely convolution, batch-normalization, activation, and pooling-layer. The sample-features extracted from both the horizontal-extraction and vertical-extraction processes were merged into a convolution-kernel of size 1×1 with a stride of 1. This work utilized the horizontal-extraction, vertical-extraction, and interleaved-extraction processes for extracting high-level noise sample-features from brain-tumor images. In the last step of high-level noise sample-feature extraction, an interpolation process is utilized, which splits the convolution kernel into final horizontal-extraction and vertical-extraction, where feature maps are constructed. The convolution-layer considered for the sample-feature extraction process is evaluated using:

$$G_k^{(o)} = \sum_{l=0}^{L} G_l^{(o-1)} * \alpha_{lk}^{(o)} + c_k^{(o)} \quad (1)$$

where $G_k^{(o)}$ denotes k^{th} feature-map constructed in o^{th} structure of CNN, $G_l^{(o-1)}$ denotes j^{th} feature-map constructed in $(o-1)^{th}$ structure of CNN, $\alpha_{lk}^{(o)}$ denotes l-channel for k^{th} convolution-kernel in o^{th} structure, $c_k^{(o)}$ denotes k^{th} biased variable for o^{th} structure, and $*$ denotes a 2-D convolutional-function. Three filtering-layers were considered for convolution, i.e., 1×1, 3×3, and 5×5, where $stride = 1$. From $G_k^{(o)}$, the feature-map from the convolution-layer is normalized by considering feature-variance with respect to the feature distribution in the intermediate layer. This is performed using batch-normalization, which is between the convolution and activation-layer. The mean average sample-feature data using batch-normalization is evaluated using:

$$\beta = \frac{1}{n}\sum_{j=0}^{n} y_j \quad (2)$$

where β represents the average sample-feature data, n represents the total sample-feature-size, and y_j represents j^{th} sample-feature-data. Also, using batch-normalization, the variance in overall sample-features within a given batch is evaluated using:

$$\gamma^2 = \frac{1}{n}\sum_{j=0}^{n}\left(y_j - \beta\right)^2 \quad (3)$$

where γ^2 denotes the variance in overall sample-features. Furthermore, the batch-normalization was applied to every feature to obtain novel sample-feature sets $\hat{y}_j$, where the average sample-feature data were initially set as 0 and the variance was set as 1. This process was achieved using:

$$\hat{y}_j = \frac{y_j - \beta}{\sqrt{\gamma^2 + \delta}} \quad (4)$$

where δ denotes a floating-trivial-point variable, in which $\delta > 0$. The last batch-normalization sample-feature extraction process is evaluated using:

$$z_j = \varphi\hat{y}_j + \omega \quad (5)$$

where ω and φ are extracted sample-features using CNN, and z_j denotes batch-normalization for the j^{th} output. To extract the best features for noise removal, the activation-layer utilized a non-linear process. Specifically, the $TanH$ activation-function was used, as more sample-features can be extracted with greater variance. Moreover, the sample-feature size was decreased by considering down-sampling feature-maps to create sequences using continuously extracted sample-features through convolution filters. Also, the max-pooling-layer was adjusted to 3×3 with a stride of 2, which was applied on all max-pooling-layers, excluding the horizontal-extraction layer $H5$ and vertical-extraction layer $V5$, as $H5$ and $V5$ provide the highest variable for every feature-map input by extracting nearby-pixel information and patterns. The average-pooling layer was utilized in the final pooling layer of $H5$ and $V5$ to down-sample feature maps to 1, thereby reducing the parameters for Fully-Connected-CNN (FCC). This approach helps in identifying noise and in reconstructing brain-tumor images.

D. Noise Removal Process

In noise removal, TL-CNN utilized the FCC, which employed the SoftMax/sigmoid process. TL-CNN used cumulated extracted sample-features from $V5$ and $H5$ to remove noise and enhance the image based on probability evaluation. The probability evaluation was conducted on the basis of noise, using:

$$P(z = 1|y) = \frac{1}{1 + f^{-a}} \quad (6)$$

$$P(z = k|y) = \frac{f^{a_k}}{\sum_{l=0}^{L} f^{a_k}} \quad (7)$$

Equation (6) represents a sigmoid process on the FCC to perform noise removal, and $P(z = 1|y)$ denotes the probability of y, which is categorized into two classes, i.e., no noise and existing noise. Equation (7) was utilized to identify noise employing the SoftMax process. The a_k in (7) denotes the FCC output for the k^{th} neuron, and $P(z = k|y)$ denotes the probability of y belonging to the noisy k^{th} group. The complete TL-CNN process is presented in Algorithm 1.

The overall parameters considered for TL-CNN are outlined in Table I, which summarizes each processing stage, including kernel sizes, activation functions, and output dimensions, providing a concise and reproducible description of the network architecture.

Algorithm 1. Noise removal and image enhancement using TL-CNN.	
Input	Noisy brain-tumor images.
Output	Noise-Free and enhanced brain-tumor images.
Step 1	Start
Step 2	Input brain-tumor images.
Step 3	Preprocess the images, i.e., resizing them into a 12 ×size, having a non-overlapping region of 8 × 8.
Step 4	Use the preprocessed image as input for TL-CNN.
Step 5	The first stage extracts multi-dimensional sample-features with noise. The sample-features are extracted using variance among nearby pixels using two directions, i.e., horizontal and vertical, considering a space-filling curved approach.
Step 6	The second stage extracts high-level noise using three extraction layers: horizontal-extraction, vertical-extraction, and interleaved-extraction.
Step 7	The third stage utilizes the Softmax/Sigmoid process for aggregating sample-features to understand multiple sample-features and removes noise, providing an enhanced image.
Step 8	Calculate the noise-free image in terms of Peak-Signal-to-Noise-Ratio.
Step 9	Get the final noise-free, improved brain-tumor images.
Step 10	Stop

E. Experimental Setup and Parameter Configuration

All experiments were conducted on a workstation equipped with an Intel Core i7 processor, 16 GB RAM, and an Intel Iris Xe graphics card. The implementation was developed using Python 3.6 and MATLAB 2018a, with the TensorFlow framework, ensuring computational efficiency, consistency, and reproducibility of the experimental results. The overall experimental parameters used for developing TL-CNN are presented in Table II.

TABLE I. TL-CNN CONFIGURATION

Stage	Layer/path	Kernel size	Activation	Output shape
Input	–	–	–	512×512×1
Stage 1	Horizontal extraction (H)	3×3, 5×5, 3×3	ReLU	512×512×16
Stage 1	Vertical extraction (V)	3×3, 5×5, 3×3	ReLU	512×512×16
Stage 2	Interleaved extraction (I)	1×1, 5×5, 5×5, 3×3	TanH	512×512×32
Stage 3	Cumulated feature aggregation	–	–	512×512×64
Stage 4	Flatten	–	–	1×1×65,536
Fully connected	Dense	–	ReLU	1024
Output	Dense	–	Sigmoid/Softmax	512×512

TABLE II. EXPERIMENTAL PARAMETERS USED FOR TL-CNN

Parameter	Value
Optimizer	Adam
Learning rate	0.0001
Batch size	16
Number of epochs	100
Maximum norm constraint	3
Convolution filter sizes	1×1, 3×3, 5×5
Activation functions	ReLU, TanH
Output activation	Sigmoid / Softmax
Input image size	512 × 512
Framework	TensorFlow
Programming language	Python 3.6, C, C++, MATLAB 2018a
Hardware	Intel Core i7 CPU, 16 GB RAM, Intel Iris Xe

III. RESULTS AND DISCUSSION

The evaluation is conducted by analyzing PSNR values across varying noise levels and by considering the average PSNR performance to assess the robustness and effectiveness of TL-CNN. For this study, the BraTS 2021 dataset [14] was utilized to evaluate the performance of TL-CNN. The dataset comprised 1,480 subjects and a total of 407,245 MRI images available in both DICOM and NIFTI formats. It included four imaging modalities: T1-weighted (T1-w), T2-weighted (T2-w), T1-weighted contrast-enhanced (T1ce), and Fluid-Attenuated Inversion Recovery (FLAIR), providing a comprehensive representation of brain anatomy and tumor characteristics. All images were preprocessed to a standard resolution of 512×512 pixels, including resizing and normalization, and non-overlapping regions of 8×8 pixels were used to preserve complete image information. The modalities were processed separately during feature extraction to allow the TL-CNN model to learn modality-specific characteristics while combining their information during high-level feature aggregation. For model training and evaluation, 70% of the images were used for training and 20% for testing, ensuring robust assessment across diverse tumor types, sizes, and spatial locations.

The results illustrated in Figure 2 highlight the effectiveness of the TL-CNN model for denoising brain tumor images. Figure 2 (a) serves as a baseline, showing the original tumor images without any noise. In Figure 2 (b), the images are degraded with a combination of different noise, which obscures critical details and makes it difficult to identify tumor regions. However, in Figure 2 (c), the TL-CNN model successfully removes all three types of noise, i.e., Rician, Gaussian, and Salt and Pepper noise, significantly enhancing image clarity. TL-CNN preserves important anatomical structures, including the tumor boundaries, while minimizing noise impact. The denoised images exhibit smoother textures and improved contrast between the brain tissue and the tumor.

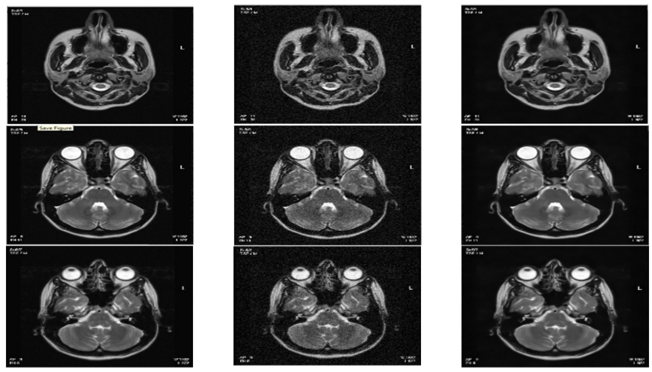

(a) (b) (c)

Fig. 2. TL-CNN model denoising results: (a) input brain-tumor image, (b) image with noise, and (c) denoised brain-tumor image.

To further contextualize TL-CNN performance, a comprehensive comparison with existing state-of-the-art methods reported in the literature is presented. As depicted in Figures 3 and 4, TL-CNN achieves a PSNR of 39.84 dB and an SSIM of 0.986, outperforming ZeroCEMR-based approaches [10], including UNetRe (PSNR = 31.7 dB, SSIM = 0.945), CUNetRe (PSNR = 34.6 dB, SSIM = 0.959), and YOLORe (PSNR = 37.82 dB, SSIM = 0.976), with relative improvements of 20.43%, 13.15%, and 5.07%, respectively, for PSNR. Additionally, TL-CNN surpasses Permutate U-Net with PCA fusion [12], which achieves a PSNR of 35.312 dB, by 11.37%. These results show the superior ability of TL-CNN to suppress noise while preserving essential anatomical details.

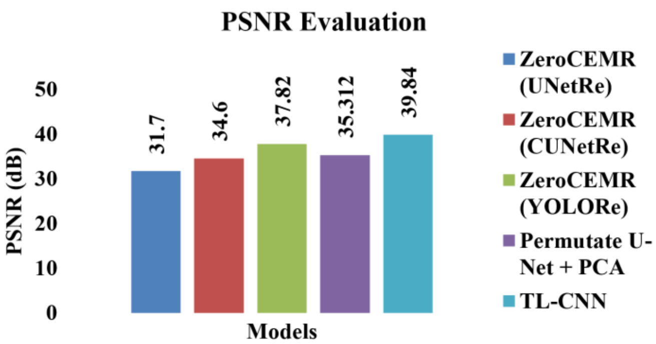

Fig. 3. PSNR comparison of the proposed TL-CNN with state-of-the-art denoising methods.

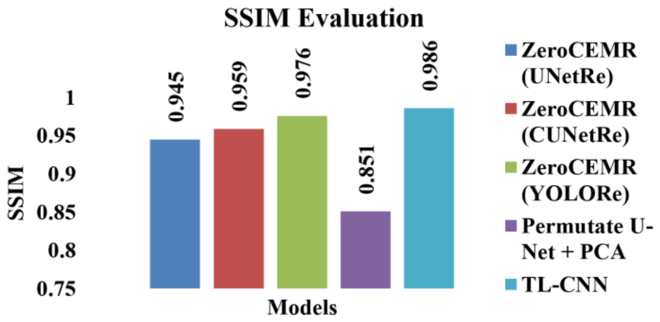

Fig. 4. SSIM comparison of the proposed TL-CNN with state-of-the-art denoising methods.

Furthermore, Table III displays the robustness of TL-CNN across varying noise levels and noise types when compared with the traditional WPT+LMMSE method [5]. Under Rician noise, TL-CNN consistently achieves PSNR values above 35 dB even at higher noise intensities, whereas WPT+LMMSE exhibits a substantial performance drop below 24 dB. Similar trends are observed for Gaussian and Salt-and-Pepper noise, where TL-CNN maintains significantly higher PSNR values across all noise levels. These findings indicate that the proposed TL-CNN not only improves noise suppression but also ensures stability and generalization under diverse and challenging imaging conditions.

TABLE III. COMPARATIVE STUDY WITH VARYING NOISE LEVELS

Ref	Models	Noise type	6%	8%	10%	12%	14%
[5]	WPT+LMMSE	Rician	28.69	27.15	25.88	24.81	23.88
		Gaussian	28.78	27.71	26.72	25.81	24.97
		Salt and Pepper	19.78	19.77	20.54	21.78	21.4
Proposed TL-CNN		Rician	39.64	38.62	37.48	36.21	35.03
		Gaussian	39.12	38.01	36.88	35.74	34.69
		Salt and Pepper	34.95	33.87	32.96	31.88	30.94

The better performance in TL-CNN can be attributed to the interleaved extraction, which enables the joint capture of spatial dependencies across both horizontal and vertical directions, allowing more effective modeling of complex and irregular noise patterns commonly present in brain MRI images. Unlike conventional single-direction or sequential feature extraction, this mechanism preserves spatial continuity and structural coherence, which is critical for maintaining tumor boundaries and fine anatomical details. By integrating information from multiple directional paths, TL-CNN improves feature robustness and reduces sensitivity to localized noise artifacts. Additionally, the combination of multi-scale convolutional filters and cumulative feature aggregation enhances contextual understanding, allowing the network to differentiate between noise and meaningful anatomical structures more effectively. This architectural design contributes directly to improved perceptual quality, structural preservation, and consistent performance across varying noise levels. Overall, compared to existing DL–based and signal-processing-based approaches reported in the literature, TL-CNN demonstrates superior robustness, higher reconstruction fidelity, and improved preservation of anatomical structures. This demonstrates its potential as a reliable and effective denoising approach for brain tumor imaging applications.

IV. CONCLUSION

This study presents a Three-Layer Convolutional Neural Network (TL-CNN), designed to enhance brain-tumor imaging by effectively suppressing noise while preserving critical anatomical structures. The proposed model integrates horizontal, vertical, and interleaved feature extraction to robustly handle complex noise patterns commonly present in medical imaging. Experimental evaluation on the Brain Tumor Segmentation (BraTS) 2021 dataset demonstrates that TL-CNN consistently outperforms existing denoising approaches, including Zero Contrast-Enhanced Magnetic Resonance Imaging (ZeroCEMR), Permutate U-Net combined with Principal Component Analysis (U-Net+PCA), and WPT+LMMSE, achieving superior Peak Signal-to-Noise Ratio (PSNR) and improved structural fidelity under varying noise conditions. Beyond numerical performance, TL-CNN enhances visual clarity and structural consistency, which are essential for accurate clinical interpretation. The proposed framework shows strong potential for integration into automated diagnostic pipelines and can be extended toward three-dimensional volumetric analysis, multimodal fusion, and downstream tasks such as tumor segmentation and classification. These capabilities position TL-CNN as a reliable and scalable solution for advanced medical imaging applications. For future work, TL-CNN can be extended to brain-tumor segmentation and classification tasks, enabling a more comprehensive automated diagnostic pipeline. Further studies could also explore performance across additional imaging modalities and noise conditions. Clinical validation studies would also provide insights into real-world applicability, ensuring TL-CNN utility in enhancing diagnostic accuracy and supporting treatment decisions. These directions will expand TL-CNN's potential as a reliable tool in medical imaging applications.

REFERENCES

[1] M. Rasool, A. Noorwali, H. Ghandorh, N. A. Ismail, and W. M. S. Yafooz, "Brain Tumor Classification Using Deep Learning: A State-of-the-Art Review," *Engineering, Technology & Applied Science Research*, vol. 14, no. 5, pp. 16586–16594, Oct. 2024, https://doi.org/10.48084/etasr.8298.

[2] M. Rasheed *et al.*, "Recognizing Brain Tumors Using Adaptive Noise Filtering and Statistical Features," *Diagnostics*, vol. 13, no. 8, Apr. 2023, Art. no. 1451, https://doi.org/10.3390/diagnostics13081451.

[3] M. Şahin, E. Şahin, E. Özdemir, F. Talu, and S. Öztürk, "Beyin Tümörü Biyopsisi Için Derin Oğrenme Tabanlı Risk Minimizasyonlu Otomatik Planlama," *Gazi Üniversitesi Mühendislik-Mimarlık Fakültesi Dergisi*, Mar. 2024, https://doi.org/10.17341/gazimmfd.1348325.

[4] "ITKTubeTK-Bullitt-Healthy MR Database." Kitware Data, 2025. [Online]. Available: https://data.kitware.com/#collection/591086ee8d777f16d01e0724/folder/58a372e38d777f0721a64dc6.

[5] N. V. T. Nguyen, T. V. Huynh, and L. V. Dang, "MRI Brain Tumor Image Enhancement Using LMMSE and Segmentation via Fast C-Means," *International Journal of Advanced Computer Science and Applications*, vol. 16, no. 5, 2025, https://doi.org/10.14569/IJACSA.2025.0160581.

[6] M. S. Elhadidy, A. T. Elgohr, M. El-geneedy, S. Akram, and H. M. Kasem, "Comparative Analysis for Accurate Multi-Classification of Brain Tumor Based on Significant Deep Learning Models," *Computers in Biology and Medicine*, vol. 188, Apr. 2025, Art. no. 109872, https://doi.org/10.1016/j.compbiomed.2025.109872.

[7] M. R. Esfandiari, "Brain Tumor MRI Dataset." Kaggle Dataset, 2025, [Online]. Available: https://www.kaggle.com/datasets/deeppythonist/brain-tumor-mri-dataset.

[8] B. Bonato, L. Nanni, and A. Bertoldo, "Advancing Precision: A Comprehensive Review of MRI Segmentation Datasets from BraTS Challenges (2012–2025)," *Sensors*, vol. 25, no. 6, Mar. 2025, Art. no. 1838, https://doi.org/10.3390/s25061838.

[9] H. Xiao, Z. Yang, T. Liu, S. Liu, X. Huang, and J. Dai, "Deep Learning for Medical Imaging Super-Resolution: A Comprehensive Review," *Neurocomputing*, vol. 630, May 2025, Art. no. 129667, https://doi.org/10.1016/j.neucom.2025.129667.

[10] Z. Guo, B. Pan, A. Lin, and N.-J. Gong, "Synthesizing Contrast-Enhanced T1 MR Image Using Multiparametric Sequences and Attention to Brain Tumor." Radiology and Imaging, Nov. 15, 2025, https://doi.org/10.1101/2025.11.14.25340220.

[11] J. S. J. Lijha and N. Muthukumaran, "CARE-MRI: Dual Channel-Hint Attention Block Integrated Residual Network for Brain MRI Image Denoising," *International Journal of Computational Intelligence Systems*, vol. 18, no. 1, Nov. 2025, Art. no. 295, https://doi.org/10.1007/s44196-025-01024-x.

[12] Y. Karuna, V. Allapakam, S. Priyanka, Sk. R. Hussian, P. Nalwaya, and S. Saritha, "Brain Tumour Segmentation in Fused MRI-PET Images with Permutate U-Net Framework," *PLOS One*, vol. 20, no. 12, Dec. 2025, Art. no. e0335952, https://doi.org/10.1371/journal.pone.0335952.

[13] C. E. Heaney, Y. Li, O. K. Matar, and C. C. Pain, "Applying Convolutional Neural Networks to Data on Unstructured Meshes with Space-Filling Curves," *Neural Networks*, vol. 175, July 2024, Art. no. 106198, https://doi.org/10.1016/j.neunet.2024.106198.

[14] U. Baid *et al.*, "RSNA-ASNR-MICCAI-BraTS-2021." The Cancer Imaging Archive, 2023, https://doi.org/10.7937/JC8X-9874.